THE JOURNAL OF BIOLOGICAL CHEMISTRY
Vol. 276, No. 42, Issue of October 19, pp. 39138–39144, 2001

Printed in U.S.A.

New Insights into the Heparan Sulfate Proteoglycan-binding Activity of Apolipoprotein E*

Received for publication, May 23, 2001, and in revised form, August 9, 2001
Published, JBC Papers in Press, August 10, 2001, DOI 10.1074/jbc.M104746200

Clare Peters Libeu‡§, Sissel Lund-Katz¶, Michael C. Phillips¶, Suzanne Wehrli¶, Maria J. Hernáiz‖, Ishan Capila‖, Robert J. Linhardt‖, Robert L. Raffaï‡§, Yvonne M. Newhouse‡, Fanyu Zhou, and Karl H. Weisgraber‡§‡‡§§**

*From the ‡Gladstone Institute of Cardiovascular Disease, San Francisco, California 94141, the §Cardiovascular Research Institute, the ‡‡Department of Pathology, University of California, San Francisco, California 94143, ¶Joseph Stokes, Jr. Research Institute, The Children's Hospital of Philadelphia, University of Pennsylvania School of Medicine, Philadelphia, Pennsylvania 19104, the ‖Departments of Chemistry, Medicinal and Natural Products Chemistry, and Chemical and Biochemical Engineering, University of Iowa, Iowa City, Iowa 52242, and the **Center for Extracellular Matrix Biology, Department of Biochemistry and Biophysics, Texas A & M University, Houston, Texas 77030*

Defective binding of apolipoprotein E (apoE) to heparan sulfate proteoglycans (HSPGs) is associated with increased risk of atherosclerosis due to inefficient clearance of lipoprotein remnants by the liver. The interaction of apoE with HSPGs has also been implicated in the pathogenesis of Alzheimer's disease and may play a role in neuronal repair. To identify which residues in the heparin-binding site of apoE and which structural elements of heparan sulfate interact, we used a variety of approaches, including glycosaminoglycan specificity assays, ^{13}C nuclear magnetic resonance, and heparin affinity chromatography. The formation of the high affinity complex required Arg-142, Lys-143, Arg-145, Lys-146, and Arg-147 from apoE and *N*- and 6-*O*-sulfo groups of the glucosamine units from the heparin fragment. As shown by molecular modeling, using a high affinity binding octasaccharide fragment of heparin, these findings are consistent with a binding mode in which five saccharide residues of fully sulfated heparan sulfate lie in a shallow groove of the α-helix that contains the HSPG-binding site (helix 4 of the four-helix bundle of the 22-kDa fragment). This groove is lined with residues Arg-136, Ser-139, His-140, Arg-142, Lys-143, Arg-145, Lys-146, and Arg-147. In the model, all of these residues make direct contact with either the 2-*O*-sulfo groups of the iduronic acid monosaccharides or the *N*- and 6-*O*-sulfo groups of the glucosamine sulfate monosaccharides. This model indicates that apoE has an HSPG-binding site highly complementary to heparan sulfate rich in *N*- and *O*-sulfo groups such as that found in the liver and the brain.

Human apolipoprotein E (apoE)[1] is a 299-residue polymorphic protein that facilitates the transport and metabolism of lipids (1). ApoE is a ligand for members of the low density lipoprotein (LDL) receptor family, heparin, and heparan sulfate proteoglycans (HSPGs) (2, 3). It is composed of two domains: a 22-kDa NH_2-terminal domain (residues 1–191) and a 10-kDa COOH-terminal domain (residues 216–299) (4). The 22-kDa NH_2-terminal domain contains the primary HSPG-binding site (residues 140–150) (5) colocalized with the LDL receptor binding site (6–8).

Binding of apoE to HSPG is an initial step in the localization of apoE-containing lipoproteins to the surface of several different types of cells (9). After localization, the apoE-containing lipoproteins are transported into the cell by pathways dependent on either the LDL receptor or the LDL receptor-related protein (LRP) or by direct uptake of an apoE-containing lipoprotein-HSPG complex (10). Binding of apoE to HSPG affects neurite extension in neurons (11, 12) and localizes secreted apoE to the surface of macrophages (13). Binding of apoE to HSPG may also play a role in Alzheimer's disease through either competition between apoE and the amyloid precursor protein (APP) for HSPG-binding sites or by modulation of the HSPG/LRP uptake pathway (14–17).

The best understood physiological role of the binding of apoE to HSPG is in lipoprotein remnant clearance. ApoE facilitates the hepatic clearance of lipoprotein remnants from the plasma through LDL receptor- and LRP/HSPG-mediated pathways. Although the LDL receptor-mediated pathway is sufficient for clearing lipoprotein remnants during fasting, the LRP/HSPG-mediated pathway is required for efficient clearance of postprandial lipoprotein remnants (15). Accumulation of lipoprotein remnants in the plasma is a major risk factor for development of atherosclerosis (18).

Several naturally occurring variants of apoE are associated with type III hyperlipoproteinemia, a disease characterized by elevated plasma lipid levels, due to the accumulations of lipoprotein remnants, and an increased risk of atherosclerosis (1). Characterization of the HSPG binding activity of these variants demonstrated that the HSPG binding activity of apoE is decreased by mutations of Arg-136 (19, 20), Arg-142 (21, 22), Arg-145 (22), and Lys-146 (23). Because the LDL receptor binding site and the HSPG-binding site overlap, predicting the physiological effect of each apoE variant is very complex. All variants known to have defective HSPG binding activity also have defective LDL receptor activity. However, moderate to severe defects in HSPG binding activity are strongly associated with dominant inheritance, increased severity, and decreased age of onset of type III hyperlipoproteinemia (9, 24).

* This work was supported by National Institutes of Health Grants HL56083 (to S. L. K. and M. C. P.), GM38060 and HL52622 (to R. J. L.), and HL41633 (to K. H. W.). The costs of publication of this article were defrayed in part by the payment of page charges. This article must therefore be hereby marked "*advertisement*" in accordance with 18 U.S.C. Section 1734 solely to indicate this fact.

§§ To whom correspondence should be addressed: Gladstone Institute of Cardiovascular Disease, P.O. Box 419100, San Francisco, CA 94141-9100. E-mail: kweisgraber@gladstone.ucsf.edu.

[1] The abbreviations used are: apoE, apolipoprotein E; LDL, low density lipoprotein; HSPG, heparan sulfate proteoglycan; DMPC, dimyristoylphosphatidylcholine; GlcN, glucosamine; IdoUA, iduronic acid; SPR, surface plasmon resonance; mS, millisiemens.

Recently, an octasaccharide that binds apoE with high affinity (K_d = 130 nM) was isolated by affinity chromatography from a heparin digest (25). This fragment is composed of four repeats of IdoUA (2-OSO_3)-$GlcNSO_3$(6-OSO_3). Although rare in most heparan sulfates (26), this disaccharide is commonly found in heparan sulfate isolated from liver (27). Therefore, the structure of the high affinity octasaccharide fragment is similar to the expected physiological ligand of apoE and thus represents a good model to study apoE and heparan sulfate interaction.

Given the physiological importance of the interaction between apoE and heparan sulfate, we have used a variety of approaches, including a glycosaminoglycan specificity assay, ^{13}C nuclear magnetic resonance (NMR), heparin column chromatography, and modeling with the high affinity binding octasaccharide, to determine which residues within the HSPG-binding site of apoE and which structural elements from the high affinity octasaccharide contribute to the interaction. From these results, we propose a model of the apoE·heparan sulfate complex.

EXPERIMENTAL PROCEDURES

Protein Production—The mutations K146Q, K146E, and R145C in apoE3[2] and R142C in apoE4 were introduced by using polymerase chain reaction to create DNA inserts that were ligated into the expression plasmid pGEX3X (28). The resulting apoE-glutathionine *S*-transferase fusion proteins were expressed in *Escherichia coli*, cleaved, and purified as described (29). The 22-kDa NH_2-terminal domain was obtained by thrombin cleavage of the full-length protein (8). The 22-kDa NH_2-terminal domains of the apoE mutants K143A, R147A, R112C (apoE4), and R158C (apoE2) and apoE3 were produced in the thioredoxin fusion protein system as described (30).

Polysaccharide Binding Assay—Bovine liver heparan sulfate, human aorta heparan sulfate, and dermatan were isolated and characterized as described (31). Bovine nasal chondroitin sulfate was provided by Dr. John Baker (Department of Biochemistry, University of Alabama at Birmingham). Heparin was partially *N*-desulfated by treating the polysaccharide with 0.04 M HCl at 50 °C for various times (32). Biotin was coupled to heparin (Sigma) and heparan sulfate (Calbiochem) by the method of Orr (33).

Microtiter wells were coated with apoE3 (200 μl, 10 μg/ml) isolated from plasma (34) and incubated at 4 °C overnight. The wells were then incubated with 1% bovine serum albumin (200 μl) to block the remaining protein binding sites. Control wells were coated with bovine serum albumin alone. Biotin-conjugated polysaccharides were diluted with phosphate-buffered saline, added with or without the competing polysaccharides to the microtiter wells, and incubated at 4 °C for 18 h. The wells were then rinsed, and alkaline phosphatase-conjugated avidin in phosphate-buffered saline was added. After incubation at 4 °C for 60 min, the wells were extensively rinsed and incubated with an alkaline phosphatase substrate (*p*-nitrophenyl phosphate; Sigma 104 phosphatase substrate) at 37 °C. Absorbance was measured at 405 nm.

Bovine liver and human aorta heparan sulfate-Sepharose gels were prepared by mixing the polysaccharide, nonactivated Sepharose 4B, and CNBr as described (35). ApoE isolated from plasma was iodinated (36) and then incubated with the polysaccharide-Sepharose gels overnight. The gel was packed into a column, washed, and eluted with sodium chloride.

NMR Measurement of the pK_a Values of the Lysines in ApoE in the Presence and Absence of the High Affinity Octasaccharide Heparin Fragment—The high affinity octasaccharide fragment of heparin was isolated and purified as described (25). ApoE3 22-kDa·DMPC complexes were prepared as described (36). The complexed apoE was reductively methylated to introduce ^{13}C methyl groups on the lysine residues (37). Then the ternary complex was prepared by adding 480 μl (1 mg/ml water) of the octasaccharide fragment to 1 ml (4 mg/ml) of reductively methylated apoE3 22-kDa·DMPC complexes. Finally, the ternary complex was diluted in 0.02 M borate in D_2O. ^{13}C NMR spectra were obtained at different pH values to characterize the influence of octasaccharide binding on the microenvironments (pK_a values) of the apoE lysine residues as previously described (38).

Preparation of DMPC Complexes for Heparin Column Chromatography—ApoE 22-kDa·DMPC complexes were prepared (36) and separated from the DMPC vesicles and free protein with a Superdex 200 column (Amersham Pharmacia Biotech) eluted with 10 mM Tris, pH 7.4, 150 mM NaCl. Except for apoE K157Q, all of the variant apoE·DMPC complexes eluted from the column within 0.5 ml of the elution volume for apoE3·DMPC, indicating that they formed complexes similar in size to the apoE3·DMPC complexes. No detectable free protein was found in the fractions containing the apoE·DMPC complexes as determined by nondenaturing polyacrylamide gel electrophoresis. The concentration of protein or protein·DMPC complex was determined by the Lowry method (39).

To measure the heparin-binding activity of the lipid-free apoE and the apoE·DMPC complexes, the lipid-free protein (60–200 μg) or the apoE·DMPC complexes (60–200 μg) were injected into a 1-ml Hi-Trap high pressure liquid chromatography heparin column (Amersham Pharmacia Biotech) equilibrated with 20 mM Tris·HCl, pH 7.4. The apoE or apoE·DMPC complexes were eluted with a linear NaCl gradient rising from 0 to 1 M NaCl in 20 column volumes. Both the flow-through and each peak in the profile were examined for apoE or apoE·DMPC complexes by nondenaturing polyacrylamide gel electrophoresis. The experiments at pH 5.0 were conducted as the experiments at pH 7.4, except that 20 mM sodium acetate was used as the buffer.

Biotinylation of Peptidoglycan Heparin—0.71 μM semipurified heparin (Celsus Inc., Cincinnati, OH) was dissolved in 400 μl of 0.1 M sodium bicarbonate and incubated with *N*-hydroxysuccinimide-LC-biotin (2 mg, 4.3 μl) dissolved in 40 μl of dimethylformamide at 4 °C for 2 h. The reaction mixture was dialyzed (3500 molecular weight cut-off) and lyophilized. The product was purified by low pressure SAX chromatography on a Dowex macroporous anion-exchange resin column (1 × 7 cm) eluted with three column volumes of water, two column volumes of 50% aqueous methanol, and three column volumes each of 0.51 and 2.7 M aqueous NaCl solution. Fractions obtained in the 0.51 and 2.7 M NaCl washes were exhaustively dialyzed against distilled water (3500 molecular weight cut-off) and freeze-dried to obtain 6 mg of biotinylated peptidoglycan heparin.

Surface Plasmon Resonance (SPR)—Streptavidin sensor chips, HEPES-buffered saline, and *N*-ethyl-*N*-(dimethylaminopropyl) carbodiimide/*N*-hydroxysuccinimide were from BIAcore (Biosensor AB, Uppsala, Sweden). All other chemicals were obtained from Sigma and were of the highest purity commercially available. SPR was measured with a BIAcore 3000 and standard system software. Buffers were filtered and deoxygenated.

Immobilization of Biotinylated Heparin on the Streptavidin Chip—A streptavidin sensor chip was pretreated with 5-μl injections of 50 mM NaOH in 1 M NaCl to remove nonspecifically bound contaminants. A 5-μl injection of biotinylated heparin (10 μg/ml) in HEPES-buffered saline (10 mM HEPES, 150 mM NaCl, 3.4 mM EDTA, pH 7.4, containing 0.005% (v/v) P-20) was made at a flow rate of 5 μl/min followed by a 10-μl injection of 2 M NaCl. The other three flow cells of the sensor chip were similarly treated with biotin, heparin, or buffer to serve as controls.

Kinetic Measurement of ApoE3 and ApoE K146Q Interaction with Heparin via SPR—ApoE3 or apoE K146Q (15 μl; concentration, 0.45–2.20 μM in HEPES-buffered saline) was injected at a rate of 5 μl/min. At the end of the sample plug, the same buffer was flowed over the sensor surface to facilitate dissociation. After a suitable dissociation time, the sensor surface was regenerated for the next sample with a 10-μl pulse of 2 M NaCl. The response was monitored as a function of time (sensogram) at 25 °C. Kinetic parameters were evaluated with BIA Evaluation software (version 3.0.2).

RESULTS

Polysaccharide-binding Assay—The glycosaminoglycan binding specificity of apoE was determined by using an enzyme-linked immunosorbent assay with bovine serum albumin as a control. Both biotinylated heparin and biotinylated bovine liver heparan sulfate bound immobilized apoE (Fig. 1) and competed effectively against biotinylated heparan sulfate for binding to immobilized apoE (Fig. 2). Heparan sulfate from human aorta, chondroitin sulfate, dermatan sulfate, and *N*-desulfated heparin were poor competitors for biotinylated heparan sulfate.

The apoE binding activities of bovine liver heparan sulfate and human aorta heparan sulfate were also measured on heparan sulfate-Sepharose affinity columns. ApoE bound strongly

[2] ApoE3 is the most common isoform of human apoE. In this paper, the notation designating the apoE variants refers to the sequence of apoE3. For example, apoE K146E is a variant of apoE that has the apoE3 sequence except for a glutamate substituted for a lysine at position 146. The two exceptions to this nomenclature for historical reasons are apoE2 (apoE R158C) and apoE4 (apoE C112R).

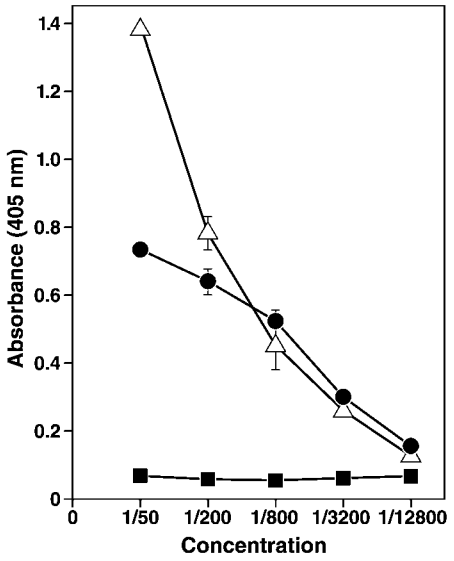

FIG. 1. **Binding of biotinylated heparin and heparan sulfate to apoE-coated microtiter wells.** Various concentrations of biotinylated heparin (△), biotinylated bovine liver heparan sulfate (●), or bovine serum albumin (■) were incubated at 4 °C with apoE-coated microtiter wells. Alkaline phosphatase-conjugated avidin was added, and the plates were incubated a second time and then washed. An alkaline phosphatase substrate was then added, and the plates were incubated at 37 °C for 25 min. Absorbance was measured at 405 nm.

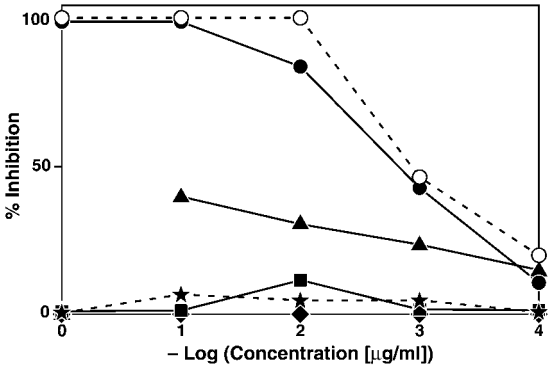

FIG. 2. **Competition between glycosaminoglycans and biotinylated heparan sulfate.** Bovine liver heparan sulfate (●), human aorta heparan sulfate (▲), dermatan sulfate (♦), chondroitin sulfate (■), *N*-desulfated heparin (★), and heparin (○) at various concentrations were incubated in apoE-coated microtiter wells with a constant concentration of biotinylated bovine liver heparan sulfate (1 ng/ml).

to a bovine liver heparan sulfate-Sepharose column but did not bind to a human aorta heparan sulfate-Sepharose column (Fig. 3). These results indicate that apoE binds with highest affinity to the highly sulfated heparan sulfate characteristic of liver HSPGs.

The Effect of the Binding of the High Affinity Octasaccharide Fragment of Heparin on the Lysine pK_a Values of ApoE—Since the most common disaccharide in bovine liver heparan sulfate is IdoUA (2-OSO_3)-GlcNSO_3(6-OSO_3) (27), we used the high affinity octasaccharide fragment of heparin as a model for the physiological ligand of apoE. The pK_a values of the eight lysines in the apoE3 22-kDa fragment were measured in the absence and presence of bound heparin octasaccharide to explore the site and mode of heparin interaction. The sequence-specific assignments of the lysine resonances in apoE3 22-kDa·DMPC discoidal complexes were derived from ^{1}H,^{13}C heteronuclear single quantum coherence NMR spectroscopy (38). The pK_a values listed in Table I were derived from the pH dependence of the chemical shifts arising from the individual

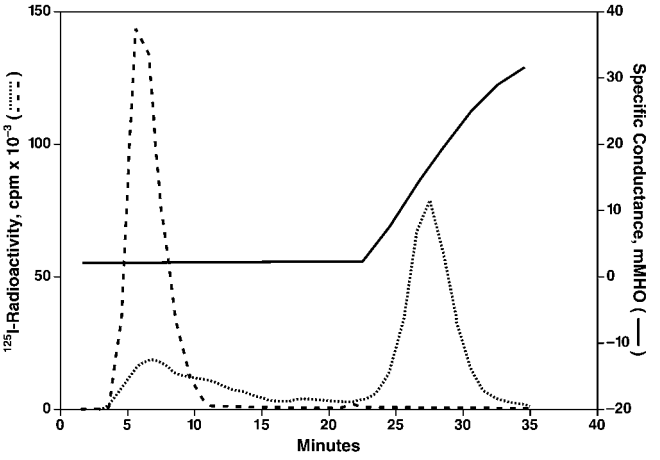

FIG. 3. **Binding of apoE to bovine liver heparan sulfate-Sepharose (*dotted line*) and human aorta heparan sulfate-Sepharose (*dashed line*).** Specific conductance (*solid line*) was used to monitor the NaCl gradient used for elution.

TABLE I
Influence of heparin on the pK_a values of lysine residues in an apoE3 22-kDa·DMPC complex

Lysine residue	pK_a[a]	
	− Octasaccharide	+ Octasaccharide
1	10.5	10.4
69	10.4	10.3
72	10.0	10.0
75	10.1	10.2
95	10.1	10.1
143	9.5	9.3
146	9.2	9.9
157	11.1	11.0

[a] The pK_a values were derived from titration curves of the type shown in Fig. 4 and are accurate to ±0.1 pH unit (37).

lysine residues. Because of the high positive electrostatic potential associated with the region surrounding residues 136–150 on helix 4 of the apoE3 22-kDa molecule, Lys-143 and Lys-146 have relatively low pK_a values of 9.5 and 9.2, respectively (38). The titration curves for Lys-143 and Lys-146 in the presence and absence of the octasaccharide are shown in Fig. 4, and the pK_a values are listed in Table I. Only the Lys-143 and Lys-146 pK_a values were significantly altered by the binding of the octasaccharide. The pK_a of Lys-143 decreased by 0.2 pH unit, whereas the pK_a of Lys-146 increased by 0.7 pH unit. These results show that the bound heparin molecule was localized to helix 4 of the apoE3 22-kDa molecule, where it interacted with Lys-143 and Lys-146 but not with Lys-157. The decrease in pK_a of Lys-143 from 9.5 to 9.3 upon interaction with heparin is consistent with the lysine amino group becoming involved in a hydrogen bond. Formation of a hydrogen bond should favor deprotonation of the amino group, leading to a decrease in pK_a. In contrast, the participation of the amino group of Lys-146 in an ionic bond with a sulfo group on heparin favors protonation of the amino group, consistent with the observed 0.7 pH unit increase in pK_a (Table I). These results also demonstrate that the microenvironments of the lysines located in helices 2 and 3 of apoE were unaffected by the binding of the octasaccharide.

Measurement of the Heparin-binding Activities of ApoE Mutants—The relative heparin-binding activities of different apoE 22-kDa variants were measured by heparin column chromatography. Because apoE is known to adopt a different tertiary conformation when bound to lipid (40), the relative heparin-binding activity of each variant was measured in both the lipid-free and the DMPC-complexed forms to determine if there

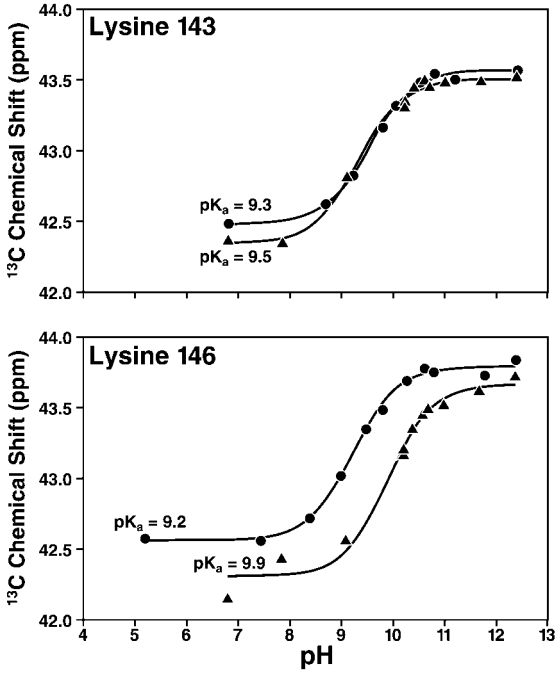

FIG. 4. **Titration curves for Lys-143 and Lys-146.** ^{13}C NMR chemical shifts (ppm) are shown as a function of pH for the resonances from selected N^{ϵ}-dimethylated lysine residues of apoE3 22-kDa·DMPC discoidal complexes in the absence (●) and presence (▲) of bound heparin. The chemical shifts were obtained from phase-sensitive ^{1}H,^{13}C heteronuclear single quantum coherence NMR spectra (37), and the pK_a values for lysines were obtained by nonlinear regression fitting to the Henderson-Hasselbalch equation.

TABLE II

Strength of the electrostatic interactions between the heparin column and the 22-kDa domain of several apoE variants and their relative heparin-binding activities at pH 7.4

Specific conductance was used to monitor the NaCl gradient used for elution and to measure the strength of the electrostatic interactions. The conductivity listed here and in Table III is the specific conductance corresponding to the peak elution position of the sample. The average deviation is 0.3 mS or 1% for all variants (n = 18 for apoE3 and n = 3 for all others); by Student's t-test for unpaired observations, $p < 0.005$ for differences greater than 2% for comparisons with apoE3 and 6% for comparisons between all other variants except apoE K157Q), except apoE K157Q, where the average deviation is 0.5 mS or 1.7% (n = 3 by Student's t-test for unpaired observations, $p < 0.005$ for differences greater than 3% for the comparison between apoE3 and apoE K157Q, 8% for the comparisons between apoE K157Q and all other variants, and 10% for the comparison between apoE K157Q free protein and apoE K157Q·DMPC).

ApoE	Free protein		Protein·DMPC	
	Conductivity	Percentage	Conductivity	Percentage
	mS	%	*mS*	%
E3	29	100	29	100
R142C[a]	19	66	17	59
K143A	16	55	17	59
K146Q	27	93	27	93
K146E	10	34	3	10
R145C	21	72	15	52
R147A	22	76	22	76
E2 (R158C)	26	90	25	86
K157Q	29	100	27	94
E4	27	94	31	106

[a] This naturally occurring variant has an additional substitution (C112R) that is also found in apoE4. This substitution has little effect on heparin-binding activity, but it alters the lipoprotein particle binding preference (28).

are significant differences. Although the heparin-binding activities of apoE K146E, apoE2 (R158C), apoE R142C, and apoE R145C have been measured by different methods (21–23), it was important for our analysis to directly compare the heparin-binding activity of these variants using the same technique on both the lipid-free and the DMPC-complexed forms.

Except for apoE K157Q, all of the variants tested had a significantly lower heparin-binding activity than apoE3, both as free protein and as protein·DMPC complexes (Table II). Large reductions in heparin-binding activity were observed for apoE R142C, apoE K143A, apoE R145C, and apoE R147A, suggesting that Arg-142, Lys-143, Arg-145, and Arg-147 all contribute to the heparin-binding site through a direct interaction with heparin.

For the apoE variants apoE4 (R112C), apoE R142C, apoE K146E, and apoE R145C, the heparin-binding activity of the free protein differs from that of the protein·DMPC complex (Table II). These results most likely reflect tertiary rearrangement of the apoE molecule upon lipid binding. Binding to DMPC requires the four-helix bundle of 22-kDa apoE to open, exposing the hydrophobic faces of its helices (40). This tertiary rearrangement is required for high affinity LDL receptor binding (36). It is likely that these apoE variants have subtle differences in their final conformations on the DMPC particle that modulate their heparin-binding activities.

In the case of Lys-146, large decreases of heparin-binding activity were observed for apoE K146E (34% of apoE3 for the lipid-free protein and 10% of apoE3 for apoE K146E·DMPC), whereas apoE K146Q had a much smaller decrease in heparin-binding activity (93% of apoE3 for both forms). Since glutamine and glutamic acid have similar shapes and capacities to form hydrogen bonds, we hypothesized that the dramatic reduction in the heparin-binding activity of apoE K146E relative to apoE K146Q is due to the ionization state of the glutamate residue at pH 7.4. The heparin-binding activities of apoE K146E and apoE K146Q are much closer at pH 5.0 (70 and 77% of apoE, respectively) (Table III). In comparison, the relative heparin-binding activity of apoE2 (apoE R158C) is insensitive to the change in pH. Therefore, the large pH-dependent differences in the relative heparin-binding activities of the Lys-146 variants are due not to a change in the behavior of the heparin column but rather to a change in the behavior of residue 146 or its microenvironment. The similarity of the heparin-binding activities of the Lys-146 variants at pH 5.0 suggests that the ionization state of the glutamate is responsible for the difference in heparin-binding activities at pH 7.4. Interestingly, the failure of the glutamine to compensate for the lysine in apoE K146Q at low pH suggests that a residue with a pK_a between pH 7.4 and 5.0 may contribute to the microenvironment in the apoE K146Q-heparin complex. His-140 and Asp-154 are possible candidates from apoE as well as the carboxyl group from one of the IdoUA units of the heparin fragment.

Determination of the Heparin-binding Affinities of ApoE3 and ApoE K146Q by Surface Plasmon Resonance—To confirm that the changes in heparin-binding activity observed with heparin column chromatography represented significant changes in heparin-binding affinity, the heparin-binding affinities of apoE3 and apoE K146Q were measured by SPR. ApoE K146Q was selected for the comparison because it has the smallest changes in heparin-binding activity as measured by heparin column chromatography of the variants with a mutation within the HSPG-binding site.

Sensograms for the binding of apoE3 and apoE K146Q to the reducing-end immobilized heparin are shown in Fig. 5. The initial portion of these curves represents buffer flowing past the sensor surface. The second and rising portions of the curve correspond to the response of the sensor surface as a sample flows past the immobilized heparin. The final portion of the curves corresponds to the dissociation of bound protein after the sample volume has finished and the buffer flows past the

TABLE III
The strength of the electrostatic interactions between the heparin column and the 22-kDa domain of apoE3, apoE K146Q, apoE K146E and their relative heparin-binding activities at pH 5.0

The average deviation is 0.3 mS or 1% ($n = 3$) for all variants (by Student's t-test for unpaired observations, $p < 0.005$ for differences greater than 6% for all comparisons in this table).

ApoE	Free protein	
	Conductivity	Percentage
	mS	*%*
E3	47	100
K146Q	37	77
K146E	33	70
ApoE2 (R158C)	42	89

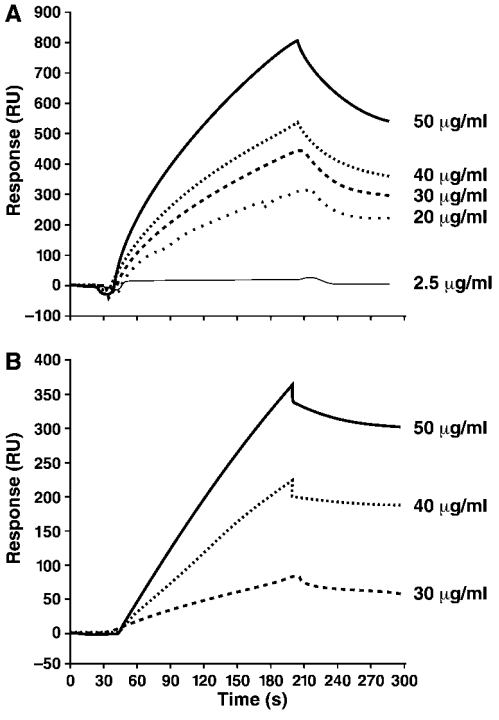

FIG. 5. **Measurement of the heparin-binding affinity of apoE3 and apoE K146Q.** *A*, SPR sensograms of apoE3 interacting with heparin. *B*, SPR sensograms of apoE K146Q interacting with heparin. Various concentrations of apoE3 or apoE K146Q were allowed to flow over a BIAcore chip with reducing-end biotinylated heparin immobilized on the surface.

sensor surface again. The resulting curves were fit according to a one-site model. The ratio of the rate of dissociation (k_d) to the rate of association (k_a) generates the dissociation constant (K_d) (Table IV). The K_d for apoE K146Q is 6.5 μM, while it is 0.32 μM for apoE3. Therefore, in apoE K146Q, the 7% decrease in the heparin-binding activity measured by heparin column chromatography corresponds to a 2000% decrease in heparin-binding affinity determined by SPR. The disparity between the heparin-binding activity and the heparin-binding affinity occurs because the two techniques measure different quantities. Heparin column chromatography primarily measures the strength of the electrostatic interactions between the protein and the column. In contrast, SPR provides a truer measurement of the heparin-binding affinity that includes contributions from hydrogen bonding and hydrophobic interactions in addition to electrostatic interactions. For example, the heparin-binding affinity of apoE4, whose heparin-binding activity is not significantly different from the heparin-binding activity of apoE K146Q or apoE2, is 0.15 μM by SPR (Table IV), which is very similar to the heparin-binding affinity of apoE3.

TABLE IV
Binding of apoE3 and apoE K146Q to heparin

	k_{on}	k_{off}	K_d
	$M^{-1}s^{-1}$	s^{-1}	μM
ApoE3	1.1×10^4	3.6×10^{-3}	0.32
ApoE K146Q	0.2×10^3	1.3×10^{-3}	6.5
ApoE4	8.4×10^4	1.3×10^{-2}	0.15[a]

[a] Data from Ref. 25.

DISCUSSION

Using a variety of techniques and approaches, we have identified residues from the HSPG-binding site of apoE and structural elements from heparan sulfate that are required for high affinity interaction. Heparin affinity chromatography demonstrated that Arg-142, Lys-143, Arg-145, Lys-146, and Arg-147 from the HSPG-binding site of apoE are required for high affinity heparin binding. In the case of Lys-143 and Arg-147, these results are the first demonstration that mutation of these residues decreases the heparin-binding activity of apoE. Our ^{13}C NMR results imply that Lys-146 participates in an ionic interaction with the heparin fragment, while Lys-143 participates in a hydrogen bond. Finally, the polysaccharide-binding assays indicate that *N*-sulfo groups on the GlcN residues of heparan sulfate are required for high affinity binding and suggest that *O*-sulfo groups also contribute to high affinity binding.

To visualize how the *N*- and *O*-sulfo groups of the octasaccharide heparin fragment might interact with the residues in the HSPG-binding site of apoE, a model of the octasaccharide fragment of heparin bound to apoE was constructed. We used the x-ray crystal structure of apoE4 (25) and a two-dimensional NMR structure of a heparin fragment chemically identical to the high affinity octasaccharide heparin fragment (41). Juxtaposition of these two structures using molecular graphics showed that the spatial pattern of the basic residues on the surface of the HSPG-binding site was highly complementary to the spatial pattern of the *N*- and *O*-sulfo groups on the heparin fragment. Only minor adjustments in the positions of the side chains of Arg-142, Arg-145, Lys-143, and Lys-146 and in the torsion angles between the monosaccharides were required to dock the heparin fragment into the HSPG-binding site and maximize the number of interactions. In this alignment, the heparin fragment interacts with Arg-136, Ser-139, His-140, Arg-142, Lys-143, Arg-145, Lys-146, and Arg-147, consistent with the reduced heparin-binding activities of the apoE variants R136H (20), R142C, K143A, R145C, K146Q, and R147A. After consideration of the conformational flexibility of the IdoUA residues (42) and further refinement of the model by manual manipulation, we obtained the model shown in Fig. 6.

This model is consistent with the results of earlier studies of the binding of heparin to apoE. For example, the trytophan fluorescence of apoE4 increases in the presence of the high affinity octasaccharide fragment (25), indicating that one of the two buried trytophans in apoE4 becomes more solvent-exposed in the complex. When the heparin fragment is docked in the orientation shown in Fig. 6, Trp-34 must be moved to a more solvent-accessible position to accommodate the monosaccharide that interacts with Arg-145. The number of ionic interactions predicted by our model is higher (eight *versus* three) than that estimated by Shuvaev *et al*. (43). However, their SPR measurements of the glycosaminoglycan binding affinity of apoE were carried out in the presence of phosphate buffer. In our hands, phosphate greatly reduces the binding affinities as determined by SPR. Since phosphate also reduces the binding of heparin fragments to an apoE3 affinity column and of apoE to the heparin affinity column (data not shown), we believe that phosphate competes with heparin for the same binding sites.

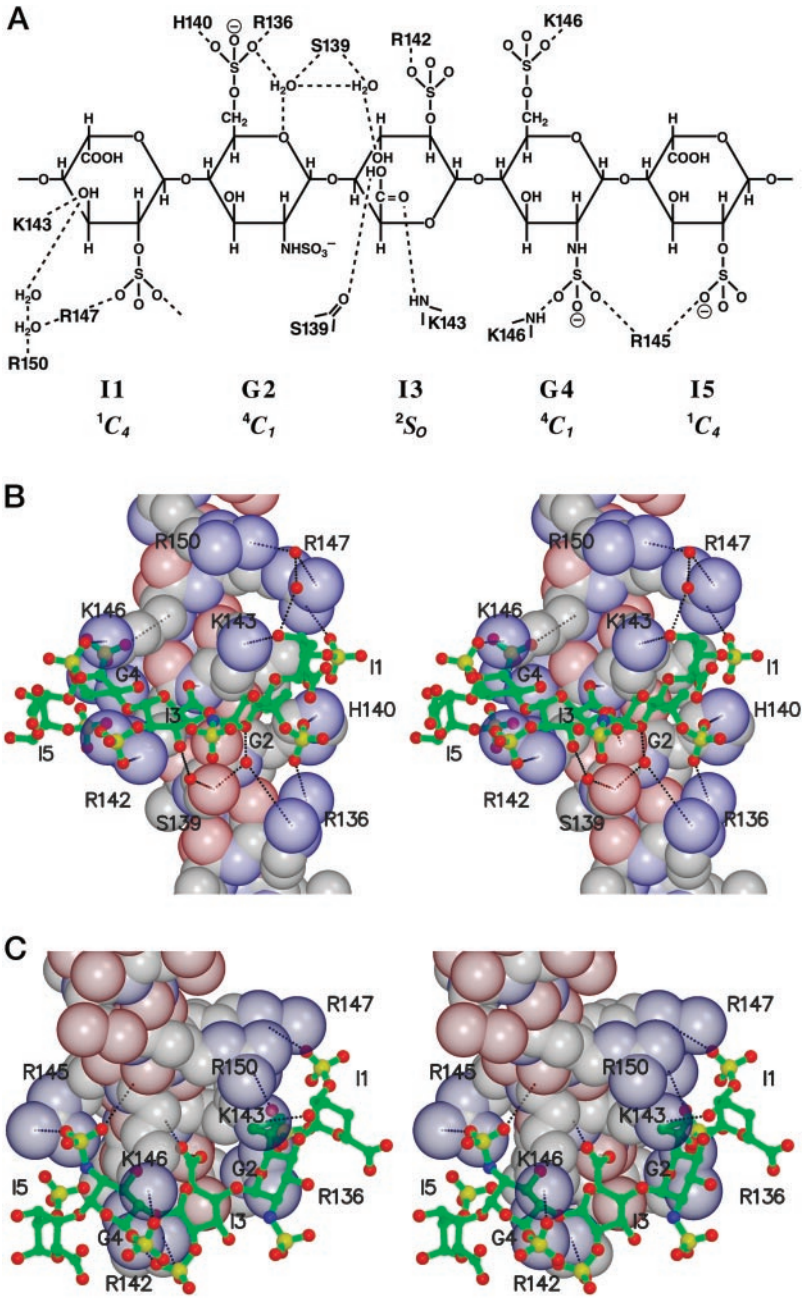

FIG. 6. **Model of the high affinity octasaccharide fragment of heparin bound to apoE.** *A*, a schematic diagram of the model illustrating the possible interactions between the heparin fragment and apoE. The monosaccharides of the heparin fragment are labeled *I* for IdoUA(2-OSO_3) and *G* for $GlcNSO_3$(6-OSO_3). The configuration of each IdoUA monosaccharide ($^1C_4$ or $^2S_0$) is also denoted. The water molecules are included in the model to indicate the presence of the two large hydrophilic pockets in the surface of the complex. *B*, a stereo view of the heparin fragment docked into the shallow groove of the HSPG-binding site of apoE. The transparent Van der Waal's surface of the protein is *colored* according to atom type: *gray* for carbon atoms, *purple* for nitrogen atoms, and *pink* for oxygen atoms. The *pink* and *purple patches* within the groove are the exposed amide nitrogens and carbonyl oxygens of the protein backbone. The heparin fragment is shown as a *ball-and-stick model* and is *colored* according to atom type: *green* for carbon, *blue* for nitrogen, and *red* for oxygen. For clarity, only the monosaccharides that interact with the protein are shown. The water molecules are shown as *red spheres*. *C*, a stereo view of the complex rotated 60° from the view in *B*. In this orientation, the 2-*O*-sulfo group of IdoUA 5 (*I5*) clearly extends into the shallow groove, where it can form a salt bridge with the amide nitrogen of Lys-146. This possible interaction suggests that the intrahelical hydrogen bond between the amide nitrogen of Lys-146 and the carbonyl oxygen of Arg-142 may be broken. Breaking of the hydrogen bond would allow the shallow groove to become wider and deeper, which would maximize the hydrophobic contribution to the free energy of binding. The stereo views were generated with MOLSCRIPT (57) and RASTER3D (58).

Our model is also well supported by the biochemical results presented in this paper. Every residue implicated by heparin column chromatography either participates directly in the complex or is potentially part of the solvation shell of the bound heparin fragment. Similarly, in the model, a hydroxyl group from the heparin fragment is hydrogen-bonded to Lys-143. The positioning of a sulfo group near Lys-146 suggests that the very low heparin-binding activity of apoE K146E originates from repulsion between the glutamate and the sulfo group. However, molecular modeling indicates that it is possible to form a salt bridge between Glu-146 and Arg-142, which would position the side chain of Arg-142 so that it blocks the shallow groove in which the heparin fragment is docked. Either possibility is consistent with the observation that the heparin binding activity of apoE K146E is approximately equivalent to that of apoE K146Q at pH 5.0.

The model is also in good agreement with the results of the polysaccharide binding assays. In the model, the basic residues in the HSPG-binding site complement all but one of the sulfo groups from the heparin fragment. Each 6-*O*-sulfo group of the $GlcNSO_3$ (6-OSO_3) units and each 2-*O*-sulfo group of the IdoUA(2-OSO_3) units interacts with either an arginine or a lysine from the HSPG-binding site. Similarly, there is an interaction between the 2-*N*-sulfo group of one of the $GlcNSO_3$(6-OSO_3) units, which is consistent with our observation that the $GlcNSO_3$ *N*-sulfo group is required for high affinity binding to apoE. Studies with acidic fibroblast growth factor (44) and basic fibroblast growth factor (45) have suggested that the pattern of interactions between the sulfo groups and the protein determines the heparan sulfate binding specificity in this family of growth factors (46). The pattern of interactions in our model suggests that apoE is specific for highly sulfated heparan sulfate. This conclusion is consistent with the higher binding affinity of apoE for liver-derived than for aorta-derived heparan sulfate, since liver-derived heparan sulfate has a higher proportion of *N*- and *O*-sulfo groups than aorta-derived heparan sulfate (27, 47, 48).

This ability to discriminate between liver-derived HSPG and HSPG in other parts of the circulatory system is critical for apoE's role in lipoprotein remnant clearance and its potential protective role in slowing the progress of atherosclerotic plaque formation. Intriguingly, the only known example of age-related changes in the pattern of sulfation of HSPG is an increase of $Glc(NSO_3)(6\text{-}OSO_3)$ in the cerebral arteries (49) and in the aorta (50), raising the possibility that apoE might have a higher affinity for aorta-derived heparan sulfate from elderly individuals than younger individuals. This higher affinity could potentially promote atherosclerosis in elderly individuals in two ways. First, significant binding between apoE-containing remnants and aorta HSPG could result in retention of the remnants in the aorta, thereby slowing clearance of the remnants by the liver. Second, binding of apoE to aorta HSPG could reduce the effectiveness of macrophage-secreted apoE to clear excess lipids from atherosclerotic lesions. ApoE-dependent reverse cholesterol transport has been suggested to be an important mechanism that retards the development of atherosclerotic lesions (13).

In addition to aging, polymorphisms or changes in physiology that decrease the proportion of *N*- or *O*-sulfo groups in liver-derived heparan sulfate might also alter lipoprotein remnant metabolism by modulating the HSPG-binding affinity of apoE-containing lipoproteins. For example, the proportion of *N*-sulfo groups on liver-derived heparan sulfate is lower in diabetic rats than normal rats (51) due to decreased activity of glucosaminyl *N*-deacetylase (52). In diabetic mice, this decrease in the sulfation of liver-derived heparan sulfate is associated with reduced lipoprotein remnant uptake (53). Our model raises the possibility that decreased glucosaminyl *N*-deacetylase activity in humans might also reduce lipoprotein remnant metabolism because of poor clearance of apoE-containing lipoproteins. However, there is no evidence that diabetes in humans decreases glucosaminyl *N*-deacetylase activity, as in the rodent model systems.

ApoE is not the only protein that binds with high affinity to polysaccharides of $IdoUA(2\text{-}OSO_3)Glc(NSO_3)(6\text{-}OSO_3)$. Lipoprotein lipase, which also plays a key role in lipoprotein metabolism in the liver, binds with high affinity to a decasaccharide composed of five $IdoUA(2\text{-}OSO_3)Glc(NSO_3)(6\text{-}OSO_3)$ units (54). In the nervous system, Aβ-(1–40) peptide and heparin-binding growth-associated molecule also bind with highest affinity to oligosaccharides of $IdoUA(2\text{-}OSO_3)Glc(NSO_3)(6\text{-}OSO_3)$ (55, 56). Both of these proteins require *N*-, 2-*O*-, and 6-*O*-sulfo groups for highest heparan sulfate binding affinity. Intriguingly, like apoE, both of these proteins have also been implicated in Alzheimer's disease or neuronal repair. However, determining the significance of the redundancy of heparan sulfate-binding sites for apoE, Aβ-(1–40), and heparin-binding growth-associated molecule will require a much better understanding of the role of the HSPG-apoE interaction in neuronal repair and Alzheimer's disease.

Acknowledgments—We thank Magnus Höök for technical advice, John Carroll and Jack Hull for graphics assistance, Stephen Ordway and Gary Howard for editorial assistance, and Brian Auerbach for manuscript preparation.

REFERENCES

1. Mahley, R. W. (1988) *Science* **240,** 622–630
2. Mahley, R. W. (1996) *Isr. J. Med. Sci.* **32,** 414–429
3. Mahley, R. W., and Rall, S. C., Jr. (2000) *Annu. Rev. Genomics Hum. Genet.* **1,** 507–537
4. Weisgraber, K. H. (1994) *Adv. Protein Chem.* **45,** 249–302
5. Weisgraber, K. H., Rall, S. C., Jr., Mahley, R. W., Milne, R. W., Marcel, Y. L., and Sparrow, J. T. (1986) *J. Biol. Chem.* **261,** 2068–2076
6. Lalazar, A., Weisgraber, K. H., Rall, S. C., Jr., Giladi, H., Innerarity, T. L., Levanon, A. Z., Boyles, J. K., Amit, B., Gorecki, M., Mahley, R. W., and Vogel, T. (1988) *J. Biol. Chem.* **263,** 3542–3545
7. Weisgraber, K. H., Innerarity, T. L., Harder, K. J., Mahley, R. W., Milne, R. W., Marcel, Y. L., and Sparrow, J. T. (1983) *J. Biol. Chem.* **258,** 12348–12354
8. Innerarity, T. L., Friedlander, E. J., Rall, S. C., Jr., Weisgraber, K. H., and Mahley, R. W. (1983) *J. Biol. Chem.* **258,** 12341–12347
9. Mahley, R. W., and Rall, S. C., Jr. (2001) in *The Metabolic and Molecular Bases of Inherited Disease* (Scriver, C. R., Beaudet, A. L., Sly, W. S., Valle, D., Childs, B., Kinzler, K. W., and Vogelstein, B., eds) 8th Ed., Vol. 2, pp. 2835–2862, McGraw-Hill Inc., New York
10. Mahley, R. W., and Huang, Y. (1999) *Curr. Opin. Lipidol.* **10,** 207–217
11. Holtzman, D. M., Pitas, R. E., Kilbridge, J., Nathan, B., Mahley, R. W., Bu, G., and Schwartz, A. L. (1995) *Proc. Natl. Acad. Sci. U. S. A.* **92,** 9480–9484
12. Bellosta, S., Nathan, B. P., Orth, M., Dong, L.-M., Mahley, R. W., and Pitas, R. E. (1995) *J. Biol. Chem.* **270,** 27063–27071
13. Lucas, M., and Mazzone, T. (1996) *J. Biol. Chem.* **271,** 13454–13460
14. Mahley, R. W. (1997) in *The Molecular and Genetic Basis of Neurological Disease* (Rosenberg, R. N., Prusiner, S. B., DiMauro, S., and Barchi, R. L., eds) 2nd Ed., pp. 1037–1049, Butterworth-Heinemann, Boston
15. Mahley, R. W., and Ji, Z.-S. (1999) *J. Lipid Res.* **40,** 1–16
16. Shuvaev, V. V., and Siest, G. (2000) *Neurosci. Lett.* **280,** 131–134
17. Van Uden, E., Kang, D. E., Koo, E. H., and Masliah, E. (2000) *Microsc. Res. Tech.* **50,** 268–272
18. Mahley, R. W., Weisgraber, K. H., and Farese, R. V., Jr. (1998) in *Williams Textbook of Endocrinology* (Wilson, J. D., Foster, D. W., Kronenberg, H. M., and Larsen, P. R., eds) 9th Ed., pp. 1099–1153, W. B. Saunders Co., Philadelphia
19. März, W., Hoffmann, M. M., Scharnagl, H., Fisher, E., Chen, M., Nauck, M., Feussner, G., and Wieland, H. (1998) *J. Lipid Res.* **39,** 658–669
20. Minnich, A., Weisgraber, K. H., Newhouse, Y., Dong, L.-M., Fortin, L.-J., Tremblay, M., and Davignon, J. (1995) *J. Lipid Res.* **36,** 57–66
21. Horie, Y., Fazio, S., Westerlund, J. R., Weisgraber, K. H., and Rall, S. C., Jr. (1992) *J. Biol. Chem.* **267,** 1962–1968
22. Ji, Z.-S., Fazio, S., and Mahley, R. W. (1994) *J. Biol. Chem.* **269,** 13421–13428
23. Mann, W. A., Meyer, N., Weber, W., Greten, H., and Beisiegel, U. (1995) *J. Lipid Res.* **36,** 517–525
24. Mahley, R. W., Huang, Y., and Rall, S. C., Jr. (1999) *J. Lipid Res.* **40,** 1933–1949
25. Dong, J., Peters-Libeu, C., Weisgraber, K. H., Segelke, B. W., Rupp, B., Capila, I., Hernáiz, L. A., LeBrun, R., and Linhardt, R. J. (2001) *Biochemistry* **40,** 2826–2834
26. Williams, K. J., and Fuki, I. V. (1997) *Curr. Opin. Lipidol.* **8,** 253–262
27. Lyon, M., Deakin, J. A., and Gallagher, J. T. (1994) *J. Biol. Chem.* **269,** 11208–11215
28. Dong, L.-M., Wilson, C., Wardell, M. R., Simmons, T., Mahley, R. W., Weisgraber, K. H., and Agard, D. A. (1994) *J. Biol. Chem.* **269,** 22358–22365
29. Dong, L.-M., Parkin, S., Trakhanov, S. D., Rupp, B., Simmons, T., Arnold, K. S., Newhouse, Y. M., Innerarity, T. L., and Weisgraber, K. H. (1996) *Nat. Struct. Biol.* **3,** 718–722
30. Morrow, J. A., Arnold, K. S., and Weisgraber, K. H. (1999) *Protein Expr. Purif.* **16,** 224–230
31. Kjellén, L., Oldberg, Å., and Höök, M. (1980) *J. Biol. Chem.* **255,** 10407–10413
32. Riesenfeld, J., Höök, M., and Lindahl, U. (1980) *J. Biol. Chem.* **255,** 922–928
33. Orr, G. A. (1981) *J. Biol. Chem.* **256,** 761–766
34. Rall, S. C., Jr., Weisgraber, K. H., and Mahley, R. W. (1986) *Methods Enzymol.* **128,** 273–287
35. Miller-Andersson, M., Borg, H., and Andersson, L.-O. (1974) *Thromb. Res.* **5,** 439–452
36. Innerarity, T. L., Pitas, R. E., and Mahley, R. W. (1979) *J. Biol. Chem.* **254,** 4186–4190
37. Lund-Katz, S., Ibdah, J. A., Letizia, J. Y., Thomas, M. T., and Phillips, M. C. (1988) *J. Biol. Chem.* **263,** 13831–13838
38. Lund-Katz, S., Zaiou, M., Wehrli, S., Dhanasekaran, P., Baldwin, F., Weisgraber, K. H., and Phillips, M. C. (2000) *J. Biol. Chem.* **275,** 34459–34464
39. Lowry, O. H., Rosebrough, N. J., Farr, A. L., and Randall, R. J. (1951) *J. Biol. Chem.* **193,** 265–275
40. Lu, B., Morrow, J. A., and Weisgraber, K. H. (2000) *J. Biol. Chem.* **275,** 20775–20781
41. Mulloy, B., Forster, M. J., Jones, C., and Davies, D. B. (1993) *Biochem. J.* **293,** 849–858
42. Conrad, H. E. (1998) *Heparin-binding Proteins*, pp. 7–60, Academic Press, Inc., San Diego
43. Shuvaev, V. V., Laffont, I., and Siest, G. (1999) *FEBS Lett.* **459,** 353–357
44. Faham, S., Hileman, R. E., Fromm, J. R., Linhardt, R. J., and Rees, D. C. (1996) *Science* **271,** 1116–1120
45. DiGabriele, A. D., Lax, I., Chen, D. I., Svahn, C. M., Jaye, M., Schlessinger, J., and Hendrickson, W. A. (1998) *Nature* **393,** 812–817
46. Faham, S., Linhardt, R. J., and Rees, D. C. (1998) *Curr. Opin. Struct. Biol.* **8,** 578–586
47. Maccarana, M., Sakura, Y., Tawada, A., Yoshida, K., and Lindahl, U. (1996) *J. Biol. Chem.* **271,** 17804–17810
48. Höök, M., Lindahl, U., and Iverius, P.-H. (1974) *Biochem. J.* **137,** 33–43
49. Murata, K., Murata, A., and Yoshida, K. (1997) *Atherosclerosis* **132,** 9–17
50. Feyzi, E., Saldeen, T., Larsson, E., Lindahl, U., and Salmivirta, M. (1998) *J. Biol. Chem.* **273,** 13395–13398
51. Kjellén, L., Bielefeld, D., and Hook, M. (1983) *Diabetes* **32,** 337–342
52. Unger, E., Pettersson, I., Eriksson, U. J., Lindahl, U., and Kjellén, L. (1991) *J. Biol. Chem.* **266,** 8671–8674
53. Ebara, T., Conde, K., Kako, Y., Liu, Y., Xu, Y., Ramakrishnan, R., Goldberg, I. J., and Shachter, N. S. (2000) *J. Clin. Invest.* **105,** 1807–1818
54. Parthasarathy, N., Goldberg, I. J., Sivaram, P., Mulloy, B., Flory, D. M., and Wagner, W. D. (1994) *J. Biol. Chem.* **269,** 22391–22396
55. Kinnunen, T., Raulo, E., Nolo, R., Maccarana, M., Lindahl, U., and Rauvala, H. (1996) *J. Biol. Chem.* **271,** 2243–2248
56. Lindahl, B., Westling, C., Giménez-Gallego, G., Lindahl, U., and Salmivirta, M. (1999) *J. Biol. Chem.* **274,** 30631–30635
57. Kraulis, P. J. (1991) *J. Appl. Crystallogr.* **24,** 946–950
58. Merritt, E. A., and Bacon, D. J. (1997) *Methods Enzymol.* **277,** 505–524